Effects of Liquid-Phase Composition on Its Migration during Liquid-Phase Sintering of Cemented Carbide

PENG FAN, JUN GUO, ZHIGANG ZAK FANG, and PAUL PRICHARD

Functionally graded composite materials (FGM composites) with a gradient of matrix phase can offer improved properties. Liquid-phase sintering is one of the approaches for making such materials with a desired gradient of the matrix phase by controlling the redistribution of the liquid phase during sintering. The present study on cemented carbide, WC-Co, demonstrates that the composition of the liquid phase (cobalt phase) is one of the key factors controlling the liquid redistribution. The dependence of the final gradient of the cobalt phase after sintering on its own chemical composition profile is quantitatively established, enabling the design and manufacture of WC-Co with a cobalt-phase-volume gradient *via* predesigned gradients of carbon content in the system.

DOI: 10.1007/s11661-009-9887-0

I. INTRODUCTION

FUNCTIONALLY graded composite materials (FGM composites) denote the composite materials with gradients of microstructural variables, such as the volume fraction of the matrix phase, the size of dispersive phase, *etc*. The gradients may spread from surfaces to the interior or from one part of a component to another. Compared to conventional homogeneous composite materials, FGM composites offer superior combinations of wear resistance, fracture toughness, high-temperature strength, thermal properties, and, hence, engineering performance.[1]

Although the potential advantages of FGM composites are easily understood, the manufacturing of FGM composites is often difficult and challenging. For some composite material systems, liquid-phase sintering is one approach that can be used to create graded microstructures, by manipulating the distribution and migration of the liquid phase during sintering. During such processes, a volume gradient of the matrix phase can either be maintained, if there is an initial gradient in the green compact, or be created during the sintering process.

During liquid-phase sintering, liquid-phase migration (LPM), also termed liquid-phase redistribution, is a physical phenomenon driven by the spontaneous tendency of the system to reduce its total interfacial energy. This phenomenon is similar to but different from the well-known capillary-driven flow in porous media, because LPM can occur in a solid-liquid two-phase system in the absence of any pore space, while the classic capillary-driven flow, resulting from the interaction among three phases (solid, liquid, and gas), relies on the existence of capillary pores.[2] In the initial stage of liquid-phase sintering, when a large volume fraction of pores exists, the liquid distribution that contributes to the densification is dependent on the capillary-driven flow, as explained by the pore-filling theory.[3] After pores are closed and eliminated with the progression of the sintering, further liquid redistribution will be controlled by the mechanism of LPM, which is, in turn, controlled by the minimization of interfacial energies; this is the subject of this study.

The driving force of LPM can be measured by liquid migration pressure, P_m. If P_m is initially inhomogeneous within a system, the liquid phase will flow from a region of low P_m to a region of high P_m. It is worth noting that the liquid migration pressure acts as an imbibition pressure or negative pressure, according to its physical effect. The liquid migration or redistribution does not stop until P_m reaches homogeneity everywhere in the system.[2,4] In other words, the liquid distribution reaches equilibrium when, and only when, the liquid migration pressure becomes homogeneous in the system. Therefore, if a factor affects the value of P_m, it will affect the equilibrium of the liquid distribution and *vice versa*. In order to control the liquid redistribution, it is necessary to first identify the key factors that affect the P_m and then quantitatively establish the dependence of the P_m as a function of these key factors.

Liquid-phase migration is an interfacial-energy-driven phenomenon. Any factor that affects the total interfacial energy in a system will affect both the liquid migration pressure and the equilibrium liquid distribution. Based on the analysis on the interfacial energy in a simplified model system,[5] liquid migration pressure in a solid/liquid mixture during sintering was proposed to be dependent of the following five factors: (1) the volume fraction of the liquid phase, u, (2) the grain size of solid phase, d, (3) the interfacial energy between the solid and the liquid phase, γ_{sl}, (4) the interfacial energy between grains of the solid phase, γ_{ss}, and (5) the coordination number of the solid grains, n_c. In many practical

PENG FAN, Research Associate, JUN GUO, Ph.D. Candidate, and ZHIGANG ZAK FANG, Associate Professor, are with the Department of Metallurgical Engineering, University of Utah, Salt Lake City, UT 84112. Contact e-mail: zak.fang@utah.edu PAUL PRICHARD, Staff Engineer, is with Kennametal, Inc., Latrobe, PA 15650-0231.

Manuscript submitted January 14, 2009.
Article published online June 23, 2009

sintering systems, the coordination number n_c is found to depend on the other three factors (u, γ_{sl}, and γ_{ss}).[6,7] For a system with a given solid phase, the solid-solid interfacial energy γ_{ss} is fixed, while the solid-liquid interfacial energy γ_{sl} varies depending on the composition of the liquid phase. In such cases, therefore, there will be only three key factors that determine the liquid migration pressure: the volume fraction of the liquid (u), the solid grain size (d), and the composition of the liquid phase.

The effects of the liquid volume fraction and solid grain size on the liquid migration pressure and liquid distribution equilibrium have been demonstrated by many experimental studies;[4,8–11] furthermore, for a composite system (WC-Co), an empirical equation describing the quantitative dependence of the liquid migration pressure as a function of the liquid volume fraction and solid grain size has been established[4] that enables the prediction of the liquid-phase distribution equilibrium for any given design of the grain size distribution. In general, liquid migrates from a region with a higher liquid volume fraction and larger solid grain size to another region with a lower liquid volume fraction or smaller grain size.

Regarding the effect of the composition of the liquid, however, there is still no concrete experimental evidence and there is a lack of comprehensive understanding. Although many experimental studies showed that equilibrium liquid distributions were affected by the total composition of the composite, there is no direct demonstration of the effect of the liquid-phase composition. For example, during the manufacturing of a functionally graded cemented tungsten carbide composite (WC-Co), the overall carbon content of the composite is a critical factor affecting the formation of the cobalt gradient.[11–16] It is well recognized that, when the overall carbon content is too high, there will be free carbon in the microstructure, while when the overall carbon content is too low, Co_3W_3C (*i.e.*, the η phase or *eta* phase) will form.[18] Although the graded structure can be engineered even in the presence of the η phase, as in the dual-property carbide process,[12,13] free carbon, or both the η phase and free carbon,[11,14–16] the involvement of Co_3W_3C or free graphite during the process makes it difficult to distinguish the effects of the volume fraction of the liquid or the composition of the liquid. The net independent effect of the liquid-phase composition is still to be demonstrated. Yet, it is technically valuable to understand and exploit the effects of the liquid composition for many applications, because the involvement of a third or more of the phases in a composite is often undesired. For example, the brittle Co_3W_3C and graphite phases are usually considered detrimental to the performance of WC-Co.

In the present study, the effect of the liquid-phase composition on the liquid migration pressure and equilibrium liquid distribution was investigated, using WC-Co as a model system. In this model system, WC is the solid phase and cobalt (with carbon and tungsten dissolved from WC grains) is the liquid phase at liquid-phase sintering temperatures. In the study, the liquid-phase (*i.e.*, cobalt phase) distributions in liquid-phase-sintered samples were examined using layered specimen configurations; each layer had a different controlled liquid-phase composition. The composition in each layer was carefully designed to ensure that other phases, except for WC and liquid cobalt, did not form during sintering, such that the effect of the liquid-phase composition on the equilibrium liquid distribution can be unambiguously determined. In this article, we will first present the experimental observations of the LPM in the specimens with a controlled liquid-phase composition. The dependence of the LPM pressure on the composition in the cobalt phase was then obtained from the experimental results. The experimental results were then used to determine the numerical factors in a model that combines the effects of the volume fraction of the liquid phase, the solid particle size, and the liquid-phase composition for WC-Co systems, enabling the prediction of the equilibrium liquid distribution and the design of the microstructural gradients for the manufacture of functionally graded WC-Co.

II. EXPERIMENTAL

The liquid-phase sintering of a tungsten carbide and cobalt (WC-Co) system is used as a model material for this study. In order to examine the effect of the liquid-phase composition on the equilibrium liquid distribution in a WC-Co system, WC-Co samples of bilayered or trilayered configurations, as shown by Figure 1, were employed, with each layer having different compositions. Figure 2 shows that the composition of each layer was chosen within the WC/liquid Co two-phase region at the sintering temperature. The compositions were so chosen that neither Co_3W_3C nor graphite would form during sintering. The composition points are labeled as $n\mathrm{Co}_{(o)}$, $n\mathrm{Co}_{(C+)}$, $n\mathrm{Co}_{(C++)}$, $n\mathrm{Co}_{(C-)}$, or $n\mathrm{Co}_{(C--)}$, for which the following is the case: (1) n denotes the Co content in weight percent; (2) the subscript (o) stands for C-stoichiometric (*i.e.*, the molar ratio of C and W is unit), the subscripts (C++) and (C+) for C-superstoichiometric or C-excess, respectively, and the subscripts

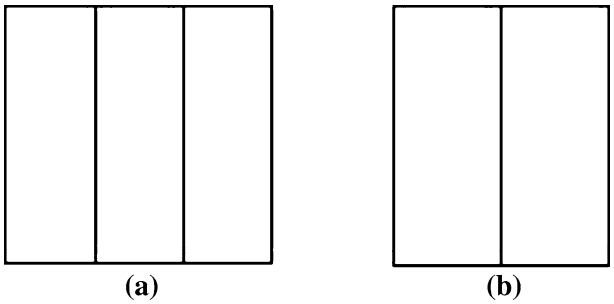

Fig. 1—Schematic of disk-shaped (*a*) trilayered and (*b*) bilayered samples. After sintering, the diameter is approximately 15 mm; the thickness of each layer in the trilayered samples is ~3 mm, while the thickness of each layer in the bilayered samples is ~4 mm. Trilayered and bilayered samples were used to qualitatively and quantitatively evaluate the effect of the liquid-phase composition on the liquid distribution equilibrium.

(C− −) and (C−) for C-substoichiometric or C-deficient respectively. The composite compositions with the same subscript have the same liquid-phase composition. It is worth pointing out that, although $n\text{Co}_{(C++)}$ and $n\text{Co}_{(C- -)}$ are located at the boundary of the WC/liquid Co two-phase region, the amount of the third phase (either Co_3W_3C phase or graphite), if any, should be very small in comparison with the majority WC phase, which, hence, would have only a negligible effect on the equilibrium distribution of the liquid phase.

For stoichiometric compositions, powders of WC and Co were mixed to prepare samples; for substoichiometric ones, WC, Co, and W were mixed; and for superstoichiometric ones, WC, Co, and graphite were used. The WC and Co powders were supplied by Kennametal, Inc., (Latrobe, PA) W by Osram Sylvania (Danvers, MA), and graphite by Alfa Aesar (Ward Hill, MA). The particle sizes were WC ~ 2 μm, Co ~ 1 μm, and W ~ 0.6 to 0.9 μm.

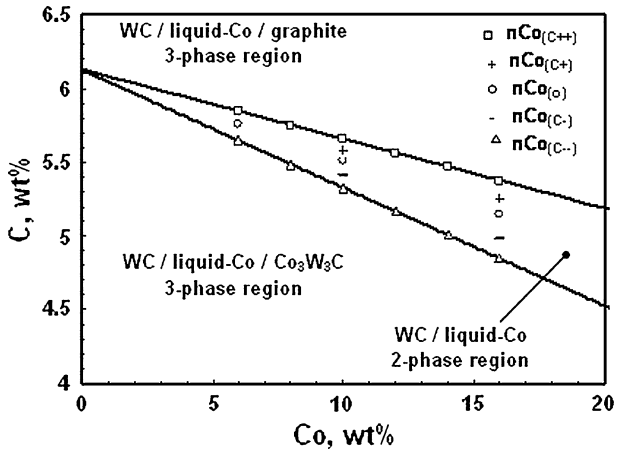

Fig. 2—Compositions used for the present study, mapped in the phase regions in the Co-W-C ternary system at the sintering temperature of 1400 °C. Note that the original isothermal section of the Co-W-C phase diagram was plotted in units of atomic percentage,[20] while it is plotted here in weight percentage.

The experimental procedure was as follows. (1) Powders were mixed together with 2 pct paraffin wax; the powder mixture was then milled in heptane in a Nalgene bottle (Nalgene Labware) containing WC balls for 14 hours on a rolling mill. (2) After milling, the powder mixture was dried in a rotary evaporator at 80 °C and then compacted at 200 MPa into layered disk-shaped samples. (3) The disk-shaped samples were dewaxed at 300 °C before liquid-phase sintering in a Red Devil vacuum furnace (R.D. Webb Company, Inc., Natick, MA), with a graphite heating element. The temperature control and variation is within ±3 °C, and the vacuum can be controlled at 10^{-2} mbar at room temperature and 10^{-1} mbar at 1400 °C. (4) Liquid-phase sintering experiments were carried out in the same vacuum furnace. The samples were heated at a rate of 10 °C/min to 1400 °C, held at that temperature for 5 minutes, and then cooled rapidly in the furnace by switching off the power. The cooling rate was approximately 40 °C/min when the temperature was above 1200 °C. The liquid-phase-sintered samples were sectioned and then polished for measuring the Co content across each layer of the sintered sample using energy-dispersive spectroscopy (EDS) techniques (EDAX, Ametek, Inc., Paoli, PA) that are integrated with scanning electron microscopy (SEM) (SM-300, Topcon Positioning Systems, Inc., Livermore, CA). The SEM images of the sintered samples, as shown in Figure 3,

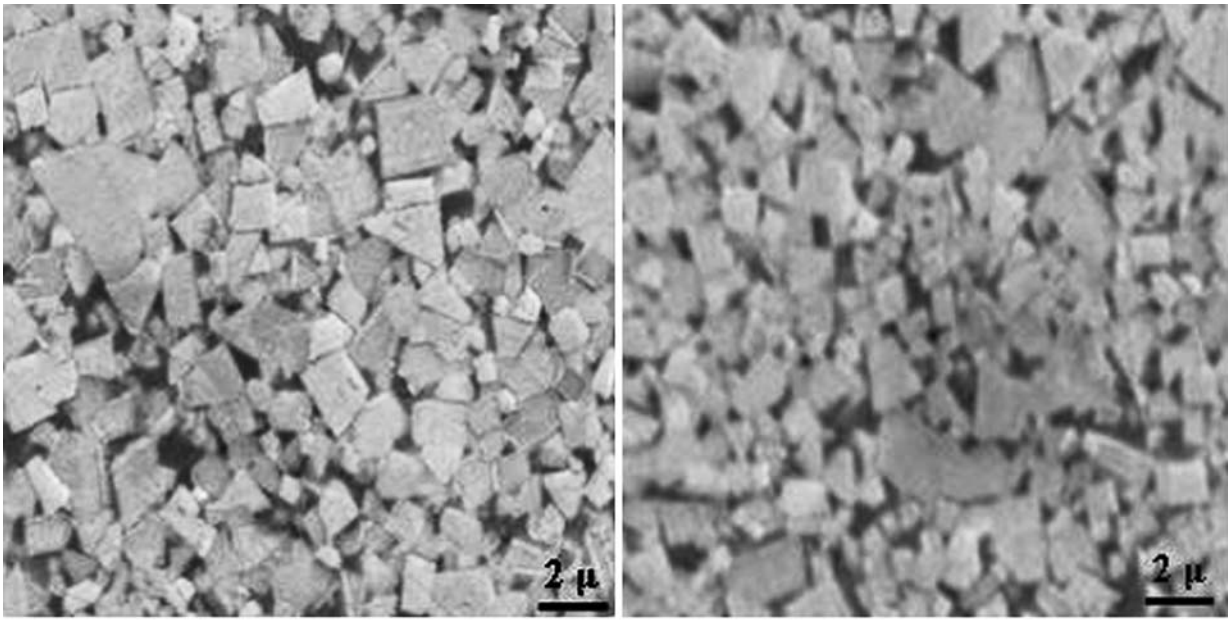

Fig. 3—Micrographs of a bilayered sample after sintering, showing no porosity.

indicated that the samples were fully densified. The WC grain size, d, was also measured on the SEM images of the samples, using the mean linear intercept length method (ASTM E112).

During analysis of the cobalt distributions of all the layered samples in this study, the effect of the grain size was assumed to be negligible, based on the fact that the grain size in any sintered layer of various compositions was 0.95 ± 0.2 μm, which was within the error range of the measurement technique. This is in agreement with the result of the reported study on the effect of the total carbon content on WC grain growth, showing very little difference in the WC grain size of the sintered samples with various C content levels when the isothermal holding time at the liquid-phase-sintering temperature was very short (Figure 6 in Reference 17).

It is also assumed that the composition of the liquid cobalt in each layer is thermodynamically at equilibrium, because the diffusion distances between the WC and Co are so small that the dissolution equilibrium is quickly obtained.[19] The equilibrium composition of the liquid phase can thus be determined based on the total composition of each layer and the isothermal section of the ternary Co-W-C phase diagram at 1400 °C.[20]

In order to understand the effects of the liquid phase, it is necessary to know the molar volumes of the primary phases. At the sintering temperature, the molar volume of WC can be calculated based on its dependence on temperature, as reported in Reference 21. The molar volume of the liquid Co phase can be determined based on the dependence of the molar volume of the liquid Co-W-C alloy on both the composition and the temperature; this was also reported in Reference 21. The total volume of liquid Co phase can then be calculated based on the Co content and the molar volume of the liquid Co. The total volume of WC was calculated based on the WC content and the molar volume of WC; the volume fraction of liquid Co phase was obtained from the total volume of the liquid Co phase and of the WC.

III. RESULTS AND DISCUSSION

A. *Experimental Observations of the Effects of Liquid-Phase Composition on Liquid Migration*

In order to qualitatively clarify the effect of the liquid-phase composition on the equilibrium distribution of the liquid phase, four trilayered samples, with each layer having the same Co but different C content levels before sintering, were sintered using the experimental procedures mentioned in Section II. The four samples can be denoted as $10Co_{(C++)}/10Co_{(o)}/10Co_{(C+)}$, $10Co_{(C--)}/10Co_{(o)}/10Co_{(C-)}$, $16Co_{(C++)}/16Co_{(o)}/16Co_{(C+)}$, and $16Co_{(C--)}/16Co_{(o)}/16Co_{(C-)}$. For example, the trilayered sample of $10Co_{(C++)}/10Co_{(o)}/10Co_{(C+)}$ has three layers. All three layers have the same initial Co content of 10 wt pct, but the left layer has the highest initial C content, the middle layer is stoichiometric, and the right layer has a carbon content between the other two layers.

After liquid-phase sintering, the Co content profiles for the two trilayered samples ($10Co_{(C--)}/10Co_{(o)}/10Co_{(C-)}$ and $16Co_{(C--)}/16Co_{(o)}/16Co_{(C-)}$), are shown in Figure 4. Obviously, a significant Co redistribution or liquid Co migration occurred during the liquid-phase sintering. The profile suggests that the liquid Co phase migrated from the stoichiometric layers toward the substoichiometric or carbon-deficient layers. This migration of liquid Co resulted in a Co content such that the stoichiometric layer decreased while the Co content in the carbon-deficient layers increased.

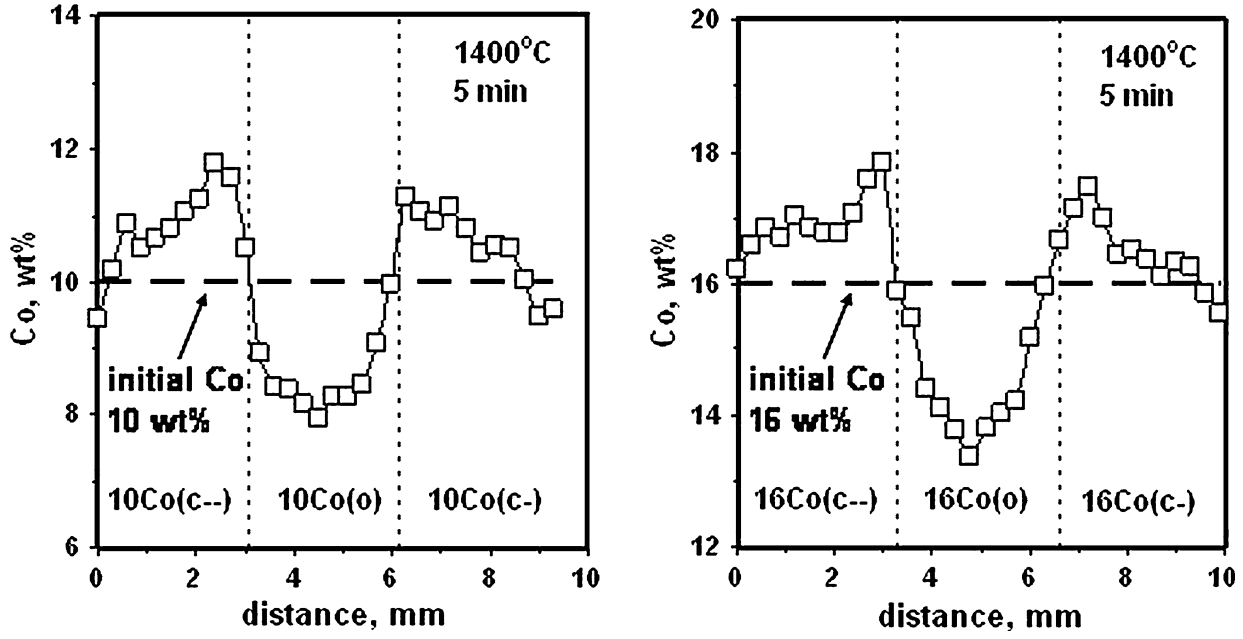

Fig. 4—The Co-content profiles after the liquid-phase sintering of the two trilayered samples, with the middle layer stoichiometric and the two side layers substoichiometric or carbon deficient.

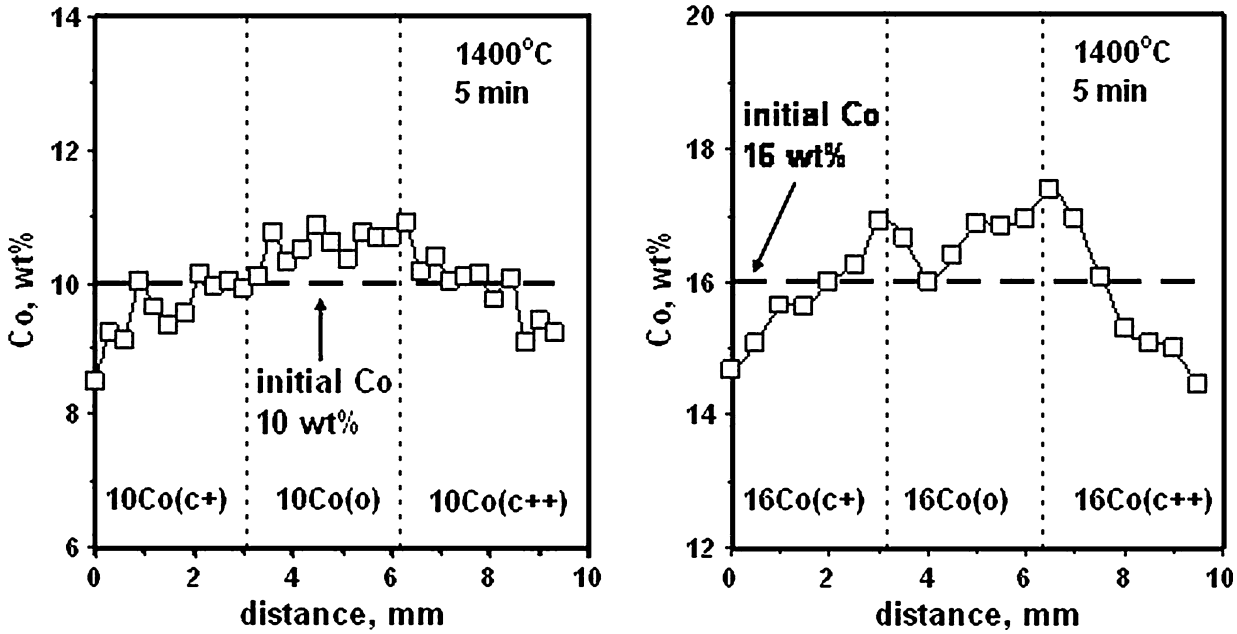

Fig. 5—The Co-content profiles after the liquid-phase sintering of the two trilayered samples, with the middle layer stoichiometric and the two side layers superstoichiometric or carbon excess.

Figure 5 shows the Co content profiles for the two trilayered samples ($10Co_{(C++)}/10Co_{(o)}/10Co_{(C+)}$ and $16Co_{(C++)}/16Co_{(o)}/16Co_{(C+)}$); in these samples, the middle layer has a stoichiometric carbon content while the two side layers are superstoichiometric (*i.e.*, carbon excess). After sintering, the Co content increased in the stoichiometric layer but decreased in the carbon-excess layer. The result suggests once again that the liquid Co phase migrated from the carbon-rich layers toward the stoichiometric layers.

The observed direction of LPM in these two cases, *i.e.*, migrating from the C-stoichiometric layer to C-deficient layers (Figure 4) or from C-excess layers to the C-stoichiometric (Figure 5) demonstrates clearly that the liquid Co phase tends to migrate from locations with a higher C content in the liquid Co phase toward the location with a lower C content in the liquid Co phase. The next step is to explain the fundamental reasons that dictate the direction of the migration process.

Earlier in this article, the redistribution of the liquid Co phase was described in terms of the change in the weight percent of Co in each layer. However, liquid-phase redistribution should be determined by the volume fraction of the liquid phase rather than by the weight percent, so the liquid Co phase distributions were replotted in terms of the volume fraction of the liquid Co phase, as shown in Figure 6 for the selected two examples, $10Co_{(C--)}/10Co_{(o)}/10Co_{(C-)}$ and $10Co_{(C++)}/10Co_{(o)}/10Co_{(C+)}$. Note that the volume fraction of the liquid Co phase depends not only on the Co content but also on the composition of the liquid Co phase that affects the density or molar volume of the liquid Co phase. The method for calculating the volume fraction of the liquid Co phase has been described in Section II.

As seen in Figure 6, if each layer maintained its initial Co content by weight percent during sintering, there would still be a difference between the layers with respect to the volume fraction of the liquid. If the liquid-phase composition had had no influence on the equilibrium of the liquid-phase distribution, the difference in the liquid volume fraction of the different layers should have decreased during sintering. To the contrary, the experimental results showed that the differences in the liquid volume fraction between the different layers increased during sintering, clearly demonstrating that the composition of the liquid phase is a critical factor affecting liquid-phase distribution or liquid migration.

The fundamental hypothesis on the effect of the liquid-phase composition is that the specific interfacial energy between the solid WC grains and the liquid phase $\gamma_{WC\text{-}Co}$ increases as the carbon content in the liquid Co phase decreases. Thus, a layer with a lower C content in the liquid phase will have a higher total interfacial energy than a layer with a higher C content in the liquid phase, provided the two layers initially have the same amount of liquid phase. In other words, the liquid migration pressure in the layer with a lower C content in the liquid Co phase is higher. The difference in the total interfacial energy or liquid migration pressure between the two layers drives the liquid phase to flow from the layer with the higher C content to the layer with the lower C content.

The experimental results of this study also reconfirm that effects of the three key factors, the volume fraction of the liquid Co phase, the grain size of WC, and the C content in the liquid Co phase, on the liquid migration during the sintering of the WC-Co system are as follows. The liquid Co phase tends to migrate from a region with a higher liquid volume fraction, larger WC grains, and a higher C content in the liquid Co phase toward another region with a lower liquid volume fraction, smaller WC grain, and lower C content in the liquid Co phase, as illustrated in Figure 7.

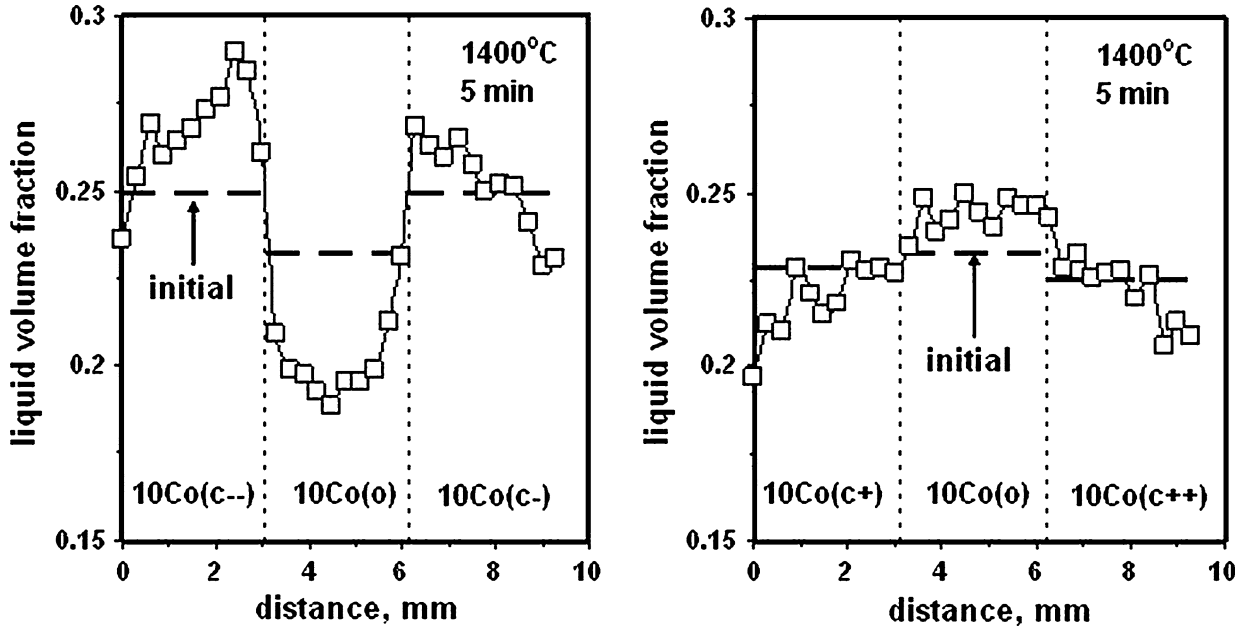

Fig. 6—Liquid volume fraction profiles after the liquid-phase sintering of the two trilayered samples.

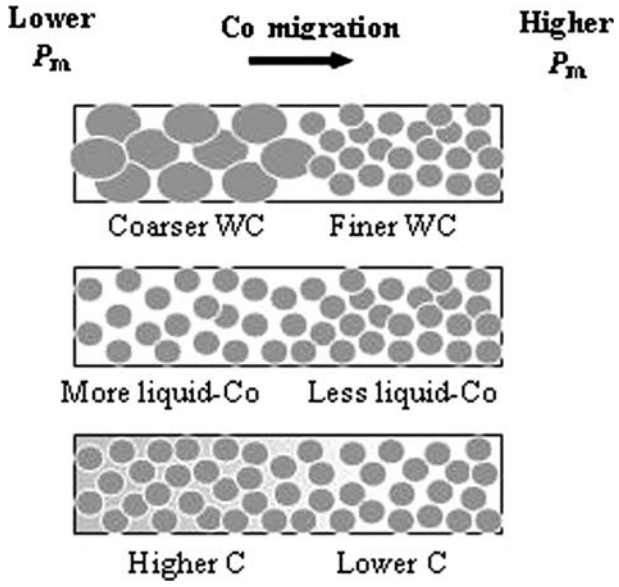

Fig. 7—Direction of Co migration, dependent on the gradients of the WC grain size, liquid Co volume, and C content in the liquid Co phase.

In Section III–B, the analysis will establish a quantitative correlation between the liquid-phase composition and the equilibrium distribution of the liquid phase.

B. *Quantitative Evaluation of the Effects of Liquid-Phase Composition on Liquid Migration*

In order to quantitatively evaluate the effect of liquid-phase composition on the liquid distribution equilibrium, a series of bilayered samples were sintered and analyzed. Before the measured results of the Co distribution in the bilayered samples can be used for the quantitative evaluation of the effects of liquid-phase composition, the following two issues have to be addressed. (1) The liquid distribution between the two layers must be at equilibrium and (2) the composition of liquid phase must be determined.

1. *Rates of liquid migration and carbon diffusion and their effects on achieving equilibrium liquid distribution*

To analyze the entire evolution of the microstructure, two separate processes must be considered: the diffusion of carbon and the migration of liquid. The kinetics of the two processes are critical to obtaining equilibrium liquid distribution. When there is an insufficient time of sintering, liquid distribution may not be equilibrated between different layers; if there is an excessively long time of sintering, the original difference in the liquid-phase composition may be completely eliminated due to diffusion. If the composition of the liquid phase is homogenized across the specimens, the liquid-phase distribution will then also be homogenized. If the homogenization process of the liquid-phase composition (*i.e.*, diffusion in the liquid) were faster than the liquid migration process, it would be difficult to examine the composition effect on the redistribution of the liquid, because the predesigned composition difference would disappear before the liquid distribution reaches equilibrium. The actual situation during the sintering of the WC-Co system, however, appears to be the opposite, *i.e.*, the liquid migration is faster than that of carbon diffusion. Otherwise, the significant redistribution of the liquid Co phase due to the original composition difference observed in the trilayered samples, as described in Section III–A, would not have occurred.

To further verify the relative kinetic effects of carbon diffusion and liquid migration in a WC-Co system, a preliminary sintering test using a bilayered sample was conducted, to determine an optimum length of time for capturing the state of equilibrium liquid distribution. The two layers, one with $6Co_{(o)}$ and another with $16Co_{(o)}$, had the same liquid-phase composition and WC grain size but different initial Co contents. After sintering, the difference in the Co content between the two layers was found to have disappeared completely, indicating that the liquid migration was indeed a fast process and a 5-minute holding at 1400 °C was sufficient for the Co distribution to reach equilibrium within the sample of the selected geometry. This result verifies that the selected sintering procedure (*i.e.*, heating at a rate of 10 °C/min to 1400 °C, holding at that temperature for 5 minutes, and then quickly cooling down in the furnace) for making samples is sufficient for the liquid distribution to reach equilibrium. The next issue is the rate of carbon diffusion and the carbon content distribution profile after 5 minutes of sintering.

2. *Determining composition of the liquid phase*

As has been pointed out, due to diffusion, the liquid composition (more specifically, the C content) difference between the two layers will decrease during sintering. Therefore, it is necessary to determine the liquid-phase composition that corresponds to the observed equilibrium distribution of the liquid phase after sintering.

For the WC-Co system, it is difficult to determine the composition change in the liquid phase at the sintering temperature. First, the measured composition of the solidified Co phase is significantly different from that of the liquid Co phase at the liquid-phase-sintering temperature, because of the precipitation of WC during cooling. Second, because the amount of the Co phase is quite small, a significant composition change within the liquid Co phase can consequently only result in a very small corresponding change in the total composition. Thus, the measured values of the total Co content and the total W content offer little information for quantitatively estimating the compositions in the liquid Co phase. Therefore, to determine the composition change *vs* sintering time, a numerical simulation is used to estimate the changes in the composition by solving the kinetic diffusion equation of carbon in liquid cobalt. It should be noted, however, that, although both carbon diffusion and liquid migration affect the composition of the liquid phase, only carbon diffusion was included in the numerical simulations that compute the liquid compositions, the justification for which is also given in the simulation that follows.

During the sintering of WC-Co with graded compositions, because the real process involves diffusion and liquid migration, a comprehensive and precise simulation of the composition changes needs to take into account the contributions from both the diffusion and liquid migration, which will be mathematically too complicated to solve and impractical for achieving the objective of this study. However, it will be shown by the following discussion that useful information can be obtained by dealing with the diffusion problem only, without taking into account the effects of liquid migration; this significantly simplifies the process and still achieves the goal of this study.

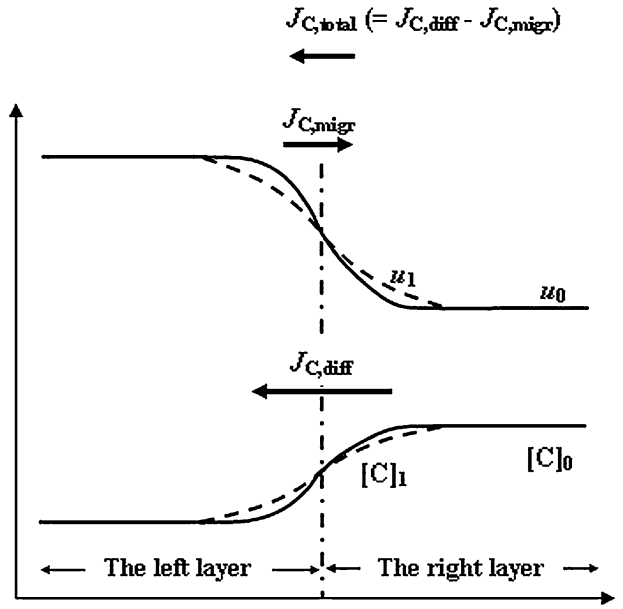

Fig. 8—Schematic of the profiles of the carbon content [C] and liquid volume fraction u in a bilayered sample, the C-transfer flux due to C diffusion ($J_{C,diff}$), and the C-transfer flux due to the liquid migration induced by the C diffusion ($J_{C,migr}$).

Referring to Figure 8, consider a bilayered sample with one layer on the left having a lower C content and the other on the right having a higher C content. Assuming that, at time t_0, corresponding to the C-content profile of the lower solid line $[C]_0$, the equilibrium liquid distribution across the bilayered sample is given by the profile of the volume fraction of the liquid Co phase as the upper solid line u_0.

As the time increases, the C content in the left layer will increase at the expense of the C content in the right layer due to a leftward carbon diffusion flux ($J_{C,diff}$). The increased C content in the left layer and the decreased C content in the right layer break the balance of the liquid distribution established based on the previous C content profile in the two layers, leading to a rightward liquid migration and, consequently, a rightward carbon flux ($J_{C,migr}$) due to this migration, indicating that C diffusion will induce a liquid migration in the opposite direction of the diffusion. Diffusion contributes positively to the composition homogenization, while the liquid migration in the opposite direction contributes negatively to the composition homogenization. The total carbon flux, $J_{C,total}$ ($=J_{C,diff} - J_{C,migr}$), is smaller than the flux that is solely due to diffusion. Therefore, composition homogenization in the real process is slower than that in a simplified simulated process that takes into account only diffusion but not liquid migration. In other words, the upper limit of the extent of the composition homogenization in the real process can be predicted from the simulation that takes into account only diffusion. The simplified simulation procedures are described as follows.

At any given temperature, the W and C contents in the liquid Co phase are interdependent with each other due to the solution equilibration of WC in the liquid Co phase, $[W]_{(in\ Co)} + [C]_{(in\ Co)} = WC_{(s)}$. Therefore, the change in the liquid-phase composition can be examined in terms of either the W or the C content. In this study, the change in the C content was examined.

The governing equation for the diffusion process is Fick's second law, which is

$$\frac{\partial[C]}{\partial t} = D_{\text{eff}}\frac{\partial^2[C]}{\partial^2 x} \qquad [1]$$

where [C] is the carbon content in the liquid Co phase (mol/m^3), t is the time (seconds), x is the distance (m), and D_{eff} is the effective diffusivity (m^2/s). It should be noted that, in a composite material in which the binder phase occupies only a small portion of the total volume, the effective diffusivity D_{eff} is much smaller than the diffusivity D in the binder phase; in addition, there is an empirical relation between them:[26] $D_{\text{eff}} = u^2 D$, where u is the volume fraction of the binder phase.

Because reliable data on the diffusivity of C in the liquid Co phase are not available in the literature, more reliable data of the diffusivity of C in the liquid Fe phase were used in this study as an approximation. The diffusivity at 1400 °C was therefore estimated to be 1.3×10^{-8} m^2/s, based on the diffusivity of C in the liquid Fe phase at 1550 °C[27] and the activation energy of the diffusivity of C in the liquid Fe phase.[28]

As an example, the change in the liquid-phase composition in a bilayered sample, $10Co_{(o)}/10Co_{(C++)}$, was simulated with the calculated profiles of the C content plotted in Figure 9. Because diffusion in solids is much slower than in liquid, the C content change in each layer should be considered solely based on the diffusion when the binder phase was at liquid state. According to the sintering procedures used in the present study, the time period during which the binder phase was in the liquid state was estimated to be 15 minutes. Therefore, the C-content profile at 15 minutes was plotted. It can be seen from the plot that the change in the C content in the middle, in an approximately 2-mm-thick zone of each 4-mm-thick layer, is quite small. In contrast, the change in the C content in the region neighboring the interlayer boundary is more significant.

Bearing in mind that the extent of the composition homogenization in the real process should be smaller than that predicted by the simulations discussed earlier, in which only diffusion was taken into account. The change in the liquid-phase composition in the middle zone of each layer during sintering should be negligibly small and thus the C content in the middle zone of each layer maintains the initial C content of each layer. Therefore, in this study, the initial liquid-phase compositions in each layer can be used for evaluating the effect of the composition of the liquid phase on the migration and the final equilibrium distribution of the liquid phase.

The simulation results indicate that the change in the liquid Co phase in the 2-mm-thick middle zone of each layer during sintering is negligibly small; thus, the liquid phase in the middle zone of each layer maintains its initial composition. Therefore, the initial compositions of the liquid phase in each layer were used to evaluate the effect of the composition on the liquid distribution.

To correlate the carbon content distribution with the liquid redistribution, bilayered samples were sintered. The bilayered samples were designed to have a different initial carbon content. After sintering, the Co content was measured across the two layers of each bilayered sample. It was found, as shown in Figure 10, that the Co content in one layer was significantly different from that in the other layer, demonstrating the effect of the C content on the liquid distribution. It was also noted that the Co contents near the interlayer boundary were different from that in the middle zone of each layer and that the Co contents near the two ends of the sample were usually lower. The former phenomenon may be attributed to the C-content change near the interlayer boundary due to the C diffusion, while the latter may have resulted from the carburization of the sample

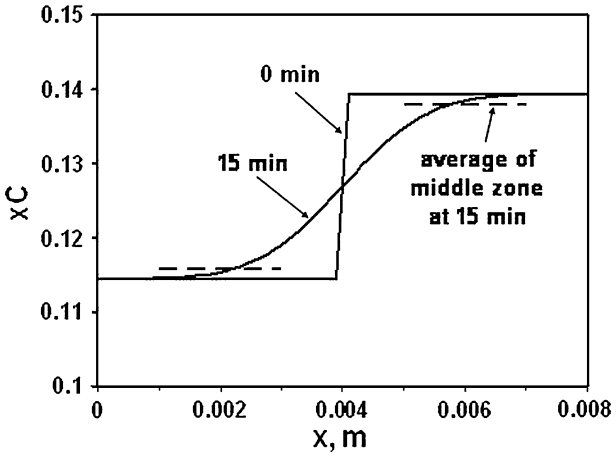

Fig. 9—Estimation of the liquid-phase composition (molar fraction of carbon) after sintering (*i.e.*, at t = 15 min), *via* simulation of the C-diffusion process in the bilayered sample, where the left side is $10Co_{(o)}$ and the right side $10Co_{(C++)}$.

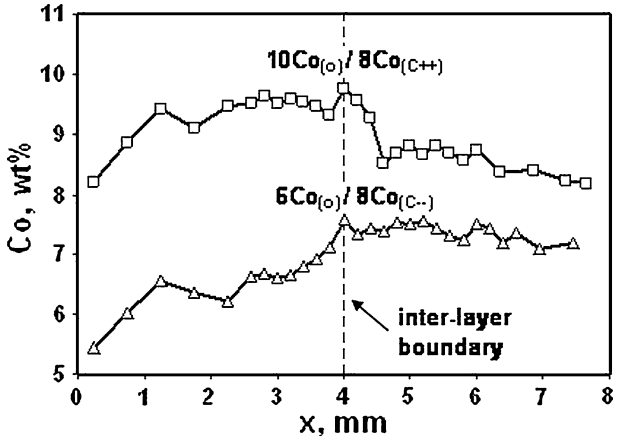

Fig. 10—Cobalt content profiles after liquid-phase sintering of the two bilayered samples.

Table I. Measured Co Distribution in Sintered Bilayered Samples and Other Relevant Data Necessary for Quantitative Evaluation of Liquid-Phase Composition Effect

Layer 1					Layer 2				
Label	Co (Wt Pct)	u	WC (μm)	$\Delta x_{[C]}$	Label	Co (Wt Pct)	u	WC (μm)	$\Delta x_{[C]}$
10Co(o)	9.43	0.2203	0.95	0	$8Co_{(C++)}$	8.67	0.1977	0.95	0.02484
10Co(o)	8.44	0.1991	0.95	0	$6Co_{(C++)}$	7.56	0.1744	0.95	0.02484
10Co(o)	11.26	0.2584	0.95	0	$16Co_{(C--)}$	14.05	0.3380	0.95	−0.01850
10Co(o)	10.68	0.2465	0.95	0	$14Co_{(C--)}$	12.68	0.3087	0.95	−0.01850
10Co(o)	9.96	0.2315	0.95	0	$12Co_{(C--)}$	11.51	0.2832	0.95	−0.01850
16Co(o)	15.89	0.3491	0.95	0	$14Co_{(C++)}$	14.03	0.3030	0.95	0.02484
16Co(o)	14.90	0.3304	0.95	0	$12Co_{(C++)}$	12.96	0.2828	0.95	0.02484
16Co(o)	13.76	0.3084	0.95	0	$10Co_{(C++)}$	12.39	0.2719	0.95	0.02484
6Co(o)	8.05	0.1906	0.95	0	$12Co_{(C--)}$	9.54	0.2390	0.95	−0.01850
6Co(o)	7.24	0.1728	0.95	0	$10Co_{(C--)}$	8.43	0.2134	0.95	−0.01850
6Co(o)	6.49	0.1561	0.95	0	$8Co_{(C--)}$	7.39	0.1889	0.95	−0.01850

surface during sintering, noting that a higher C content induces a lower Co content. In order to minimize error in the evaluation of the composition effect, only the Co contents measured in the 2-mm-thick middle zone of each layer were used to calculate the average Co content in each layer. In total, 11 bilayered samples were sintered for the quantitative evaluation of the composition effect on liquid distribution. The results are listed in Table I.

3. *Modeling the dependence of liquid migration pressure on carbon content*

As described in Section I, the effects of the key factors on the equilibrium liquid distribution are manifested on the liquid migration pressure. To obtain a quantitative understanding of those effects, the dependence of the liquid migration pressure on the key factors must be established.

Based on the experimental studies by Lisovsky[8,22–24] on the dependence of the liquid migration pressure on the liquid volume fraction and the study by the present authors[4] on the dependence of the liquid migration pressure on the WC grain size, the following empirical equation is available:

$$P_m = 2048[(1/u - 1)^{1/3} - 1.41u]/d^{0.4} \qquad [2]$$

where P_m is the liquid migration pressure (Pa), u is the liquid Co volume fraction, and d is the WC particle size (linear intercept length) (m).

Equation [2] is satisfactory when applied to WC-Co systems with a stoichiometric carbon content. In order to describe the effect of the carbon content when WC-Co is not at stoichiometry, however, the equation has to be modified to include additional terms. Therefore, the following equation is proposed in this study:

$$P_m = 2048(1 + b_1\Delta x_{[C]} + b_2\Delta x_{[C]}^2) \times [(1/u - 1)^{1/3} - 1.41u]/d^{0.4} \qquad [3]$$

where $\Delta x_{[C]}$ is the difference in the molar fraction of C in the liquid Co phase with respect to stoichiometry and b_1 and b_2 are empirical coefficients to be determined from the experimental results. As noted earlier, bilayered samples were used in this study to determine the numerical coefficients.As shown in Table I, the bilayered samples were designed such that the C content in layer 1 was stoichiometric, *i.e.*, $(\Delta x_{[C]})_1 = 0$, while the C content in layer 2 was nonstoichiometric, *i.e.*, $(\Delta x_{[C]})_2 \neq 0$. The WC particle sizes in the two layers were the same, *i.e.*, $d_1 = d_2$. Subscripts 1 and 2 denote layers 1 and 2, respectively. As explained in Section I, when the equilibrium liquid distribution was reached in the WC-Co bilayered sample, the liquid migration pressures in the two layers would equalize, *i.e.*, $(P_m)_1 = (P_m)_2$, which results in the following equation based on Eq. [3]:

$$[(1/u_1 - 1)^{1/3} - 1.41u_1] = [1 + b_1(\Delta x_{[C]})_2 + b_2(\Delta x_{[C]})_2^2][(1/u_2 - 1)^{1/3} - 1.41u_2] \qquad [4]$$

Rearranging this equation leads to

$$f = \frac{(1/u_1 - 1)^{1/3} - 1.41u_1}{(1/u_2 - 1)^{1/3} - 1.41u_2} = 1 + b_1(\Delta x_{[C]})_2 + b_2(\Delta x_{[C]})_2^2 \qquad [5]$$

Using Eq. [5], b_1 and b_2 were obtained by linear regression based on the data of the liquid Co volume fraction (u) and the molar fraction difference of the C in the liquid Co phase with respect to stoichiometry ($\Delta x_{[C]}$), as listed in Table I. The results were $b_1 = -9$ and $b_2 = 155$.

The dependence of P_m as a function of u, d, and $\Delta x_{[C]}$ is thus expressed as

$$P_m = 2048(1 - 9\Delta x_{[C]} + 155\Delta x_{[C]}^2) \times [(1/u - 1)^{1/3} - 1.41u]/d^{0.4} \qquad [6]$$

where P_m is the liquid migration pressure (Pa); u is the liquid Co volume fraction; $\Delta x_{[C]}$ is the difference in the molar fraction of C in the liquid Co phase with respect to stoichiometry; and d is the WC particle size (linear intercept length) (m).

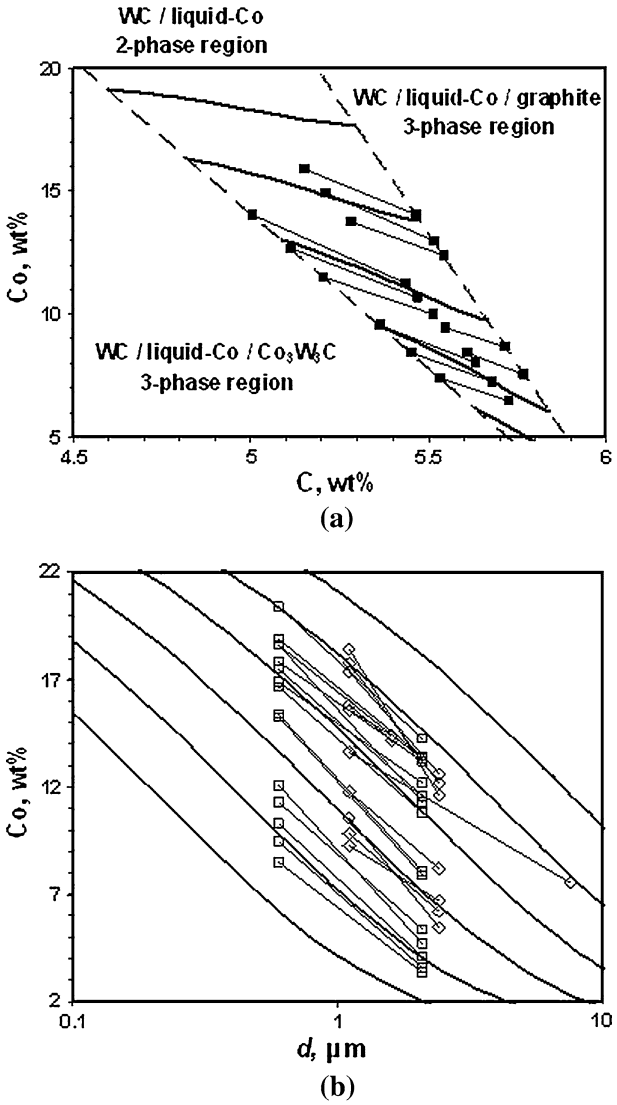

Fig. 11—Comparison of measured liquid distribution equilibrium (straight thin lines connecting two squared or diamond marks) with the iso-P_m contours (thick solid lines) predicted by the model (Eq. [6]) (*a*) as a function of Co and C contents at a fixed WC grain size of 0.95 μm and (*b*) as a function of the Co content and WC grain size at a fixed C content in the liquid Co phase corresponding to the stoichiometric composition. The experimental data in (a) were from the present study, while those in (b) were from Ref. 4 (diamond points) and Ref. 25 (squared points).

To demonstrate the reliability of this model, iso-P_m contour lines calculated from Eq. [6] were plotted in Figure 11. The measured equilibrium liquid distribution for various bilayered samples in this study and in other reported studies[4,25] were included for comparison. The equilibrium liquid distribution should, in theory, follow the iso-P_m contour lines. The line that connects each pair of layers in a sintered bilayered sample is an observed equilibrium of liquid distribution. Figure 11 shows a good agreement between the measured connecting lines and the iso-P_m contour lines, indicating that the model predicts the equilibrium with reasonable accuracy under the following given conditions: (1) 1400 °C, (2) the compositions of WC-Co are such that

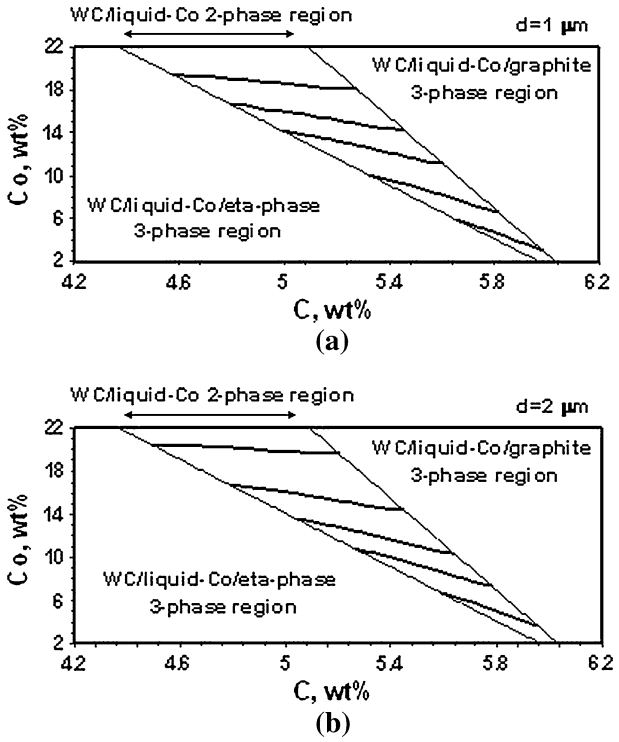

Fig. 12—Iso-P_m contour lines as a function of the Co and C contents at the fixed WC grain sizes of (*a*) 1 and (*b*) 2 μm.

there is neither *eta* phase nor graphite at the temperature, and (3) the WC grain size after sintering is from 0.6 to 7.5 μm.

C. *Application of Model to Design of Co Gradient by Controlling C Content and WC Particle Size*

The establishment of the dependence of the liquid migration pressure as a function of the volume fraction of the liquid Co phase, C content, and WC particle size serves as a tool for the custom designing and manufacturing of WC-Co FGM composites. As mentioned in Section I, the equilibrium liquid distribution is reached when the liquid migration pressure is uniform throughout the composite material. For any given value of the liquid migration pressure, the volume fraction of the liquid Co phase varies with the C content and WC particle size. A desired Co gradient can be acquired by predesigning a suitable gradient of the C content and WC particle size. This approach can be readily used to design various bilayered, multilayered, or continuously graded structures of WC-Co.

To illustrate the utility of Eq. [6], contour plots of P_m as a function of the Co and C content at constant WC particle sizes of 1 and 2 μm are computed using Eq. [6] and plotted in Figure 12. Any two points on the same contour line have the same liquid migration pressure and thus can represent the final or equilibrium Co and C contents in a bilayered WC-Co structure. Therefore, these contour line plots can be used to custom design a WC-Co composite with a Co gradient by varying the C gradient.

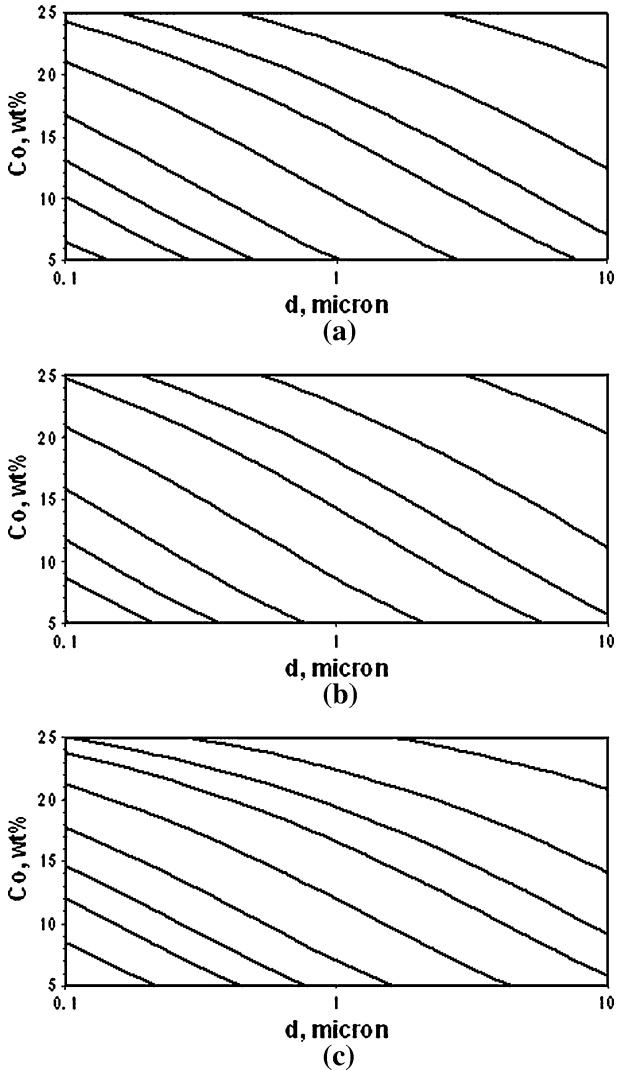

Fig. 13—Iso-P_m contour lines as a function of the Co and WC grain size at fixed liquid-phase compositions of (*a*) stoichiometry ($Co_{(o)}$), (*b*) superstoichiometry ($Co_{(C++)}$), and (*c*) substoichiometry ($Co_{(C--)}$).

Similarly, contour plots of P_m as a function of the Co content and WC particle size at stoichiometric, superstoichiometric, and substoichiometric C compositions are also computed using Eq. [6] and plotted in Figure 13. These contour line plots can be used to design and fabricate WC-Co composites with a Co gradient by varying the WC particle size gradient.

It is possible to design and fabricate WC-Co with a Co gradient by varying both the C content and WC particle sizes. For this purpose, the contour surfaces (rather than the contour lines) of P_m as a function of the Co content, C content, and WC particle size must be computed and plotted. However, an alternative to using contour surfaces is to numerically solve Eq. [6]. Suppose that a WC-Co bilayered structure with the liquid Co volume fractions of u_1 and u_2 needs to be fabricated by varying both the C content and WC particle size in each layer. According to $(P_m)_1 = (P_m)_2$ and Eq. [6], it is necessary to have

$$\begin{aligned}&[1 + b_1(\Delta x_{[C]})_1 + b_2(\Delta x_{[C]})_1^2][(1/u_1 - 1)^{1/3} - 1.41u_1]/d_1^{0.4} \\ &\quad = [1 + b_1(\Delta x_{[C]})_2 + b_2(\Delta x_{[C]})_2^2] \\ &\qquad \times [(1/u_2 - 1)^{1/3} - 1.41u_2]/d_2^{0.4} \end{aligned} \quad [7]$$

Solving Eq. [7] with the available values of u_1 and u_2 can lead to a series of solutions of $((\Delta x_{[C]})_1, d_1; (\Delta x_{[C]})_2, d_2)$. Based on practical considerations, one can select one solution among multiple solutions for use in designing the desired graded WC-Co.

IV. SUMMARY

In the present study, the effect of the liquid-phase composition on the liquid migration and equilibrium liquid distribution during the liquid-phase sintering of composite materials was investigated. The investigation was carried out by examining the liquid distribution in the liquid-phase-sintered specimens with layered configurations. Each layer of the specimen was designed to have different liquid-phase compositions. The experimental results clearly demonstrated that the liquid-phase composition is one of the key factors controlling the LPM and liquid equilibrium distribution. The effect of the liquid-phase composition on the liquid distribution equilibrium was attributed to the change in the interfacial energy at the solid-liquid interface.

A composite material, WC-Co, was used as a model system in this study. It was found that the liquid phase migrated from the region with the higher C content in the liquid phase toward that with the lower C content. The dependence of the liquid migration pressure (the driving force of the liquid redistribution) on the composition of the liquid phase was obtained based on the experimental results. In combination with a previously reported study on the effects of the liquid volume fraction and solid grain sizes, the dependence of the LPM as a function of all three key factors (the liquid volume fraction, solid grain size, and liquid-phase composition) was quantitatively established for this material system, enabling quantitative predictions of the equilibrium liquid distribution and the design of the desired functionally graded WC-Co.

ACKNOWLEDGMENTS

The authors acknowledge the financial support for this research provided by multiple sources, including the United States Department of Energy with the Grant Number DE-FC36-04GO14041, the State of Utah Centers of Excellence Program, and Kennametal, Inc., at various times in the past six years.

REFERENCES

1. S. Suresh and A. Mortensen: *Fundamentals of Functionally Graded Materials*, The Institute of Materials, London, 1998.
2. P. Fan, Z.Z. Fang, and H.Y. Sohn: *Acta Mater.*, 2007, vol. 55, pp. 3111–19.

3. Y.P. Kim, S.W. Jung, and S.J.L. Kang: *J. Am. Ceram. Soc.*, 2005, vol. 88, pp. 2106–09.
4. P. Fan, O. Eso, Z.Z. Fang, and H.Y. Sohn: *Int. J. Refract. Met. Hard Mater.*, 2008, vol. 26, pp. 98–105.
5. F. Delannay, D. Pardon, and C. Colin: *Acta Mater.*, 2005, vol. 53, pp. 1655–64.
6. R.M. German: *Liquid Phase Sintering*, Plenum Press, New York, NY, 1985.
7. A.N. Niemi, L.E. Baxa, J.K. Lee, and H. Courtney: *Modern Developments in Powder Metallurgy*, Metal Powder Industries Federation, Princeton, NJ, 1981, pp. 483–95.
8. A.F. Lisovsky: *Int. J. Heat Mass Transfer*, 1990, vol. 33, pp. 1599–1603.
9. C. Colin, L. Durant, N. Favrot, J. Besson, G. Barbier, and F. Delannay: *Proc. 13th Planesse Seminar*, Plansee Group, Reutte, Austria, 1993, vol. 2, pp. 522–36.
10. S. Put, J. Vleugels, and Van der Biest: *Scripta Mater.*, 2001, vol. 45, pp. 1139–45.
11. Z.Z. Fang and O. Eso: *Scripta Mater.*, 2005, vol. 52, pp. 785–91.
12. U.K.R. Fisher, E.T. Hartzell, and J.G.H. Akerman: U.S. Patent No. 4,743,515, 1985.
13. Y. Liu, H. Wang, Z. Long, P.K. Liaw, J. Yang, and B. Huang: *Mater. Sci. Eng., A*, 2006, vol. 426, pp. 346–56.
14. O. Eso, Z.Z. Fang, and A. Griffo: *Int. J. Refract. Met. Hard Mater.*, 2005, vol. 23, pp. 233–41.
15. O. Eso, Z.Z. Fang, and A. Griffo: *Int. J. Refract. Met. Hard Mater.*, 2007, vol. 25, pp. 286–92.
16. O. Eso, P. Fan, and Z.Z. Fang: *Int. J. Refract. Met. Hard Mater.*, 2008, vol. 26, pp. 91–97.
17. V. Chabretou, C.H. Allibert, and J.M. Missiaen: *J. Mater. Sci.*, 2003, vol. 38, pp. 2581–90.
18. G.S. Upadhyaya: *Cemented Tungsten Carbides: Production. Properties and Testing*, Noyes Publications, Park Ridge, NJ, 1998.
19. S. Haglund and J. Agren: *Acta Mater.*, 1998, vol. 46, pp. 2801–07.
20. A.E. Mahale: *Phase Diagrams for Ceramists*, The American Ceramic Society, Westerville, OH, 1994, vol. X.
21. B. Uhrenius: *Int. J. Refract. Met. Hard Mater.*, 1993–1994, vol. 12, pp. 121–27.
22. A.F. Lisovsky: *Powder Metall. Int.*, 1987, vol. 19, pp. 18–21.
23. A.F. Lisovsky: *Migration of Metal Melts in Sintered Composite Bodies*, Naukova Dumka, Kiev, 1984.
24. A.F. Lisovsky: *Int. J. Refract. Met. Hard Mater.*, 1989, vol. 8, pp. 133–36.
25. C. Colin, V. Guipont, and F. Delannay: *Metall. Mater. Trans. A*, 2007, vol. 38A, pp. 150–58.
26. P. Grathwohl: *Diffusion in Natural Porous Media*, Kluwer Academic Publishers, Norwell, MA, 1998, p. 34.
27. T. Iida and R.I.L. Guthrie: *The Physical Properties of Liquid Metals*, Oxford University Press, New York, NY, 1988, p. 223.
28. P. Kubicek and T. Peprica: *Int. Met. Rev.*, 1983, vol. 28, pp. 131–57.